RSC Advances

Histidine-mediated synthesis of chiral fluorescence gold nanoclusters: insight into the origin of nanoscale chirality

Journal:	*RSC Advances*
Manuscript ID:	RA-ART-06-2015-010985.R1
Article Type:	Paper
Date Submitted by the Author:	08-Jul-2015
Complete List of Authors:	Liu, Zhongde; Southwest University, Guo, Yanjia; Southwest University, Zhao, Xi Juan; Southwest University, Long, Tengfei; Southwest University, College of Pharmaceutical Sciences Lin, Min; Southwest University, College of Pharmaceutical Sciences Huang, Cheng Zhi; Southwest University, Collge of Pharmaceutical Sciences

Journal Name

RSCPublishing

ARTICLE

Histidine-mediated synthesis of chiral fluorescence gold nanoclusters: insight into the origin of nanoscale chirality

Cite this: DOI: 10.1039/xoxxoooooox

Received ooth January 2012,
Accepted ooth January 2012

DOI: 10.1039/xoxxoooooox

www.rsc.org/

Yanjia Guo [a], Xijuan Zhao [b], Tengfei Long [a], Min Lin, Zhongde Liu [a]*, Chengzhi Huang [a]

Despite a significant surge in the number of investigations into the chirality at the nanoscale, there is currently only limited knowledge about the chiral origin and their potential applications. Here, we have succeeded in preparing a pair of gold nanocluster enantiomers, in which the histidine (His) enantiomers serve as both the reducing agent and the stabilizing ligand. Origins of the optical activity are discussed from the viewpoint of the intrinsically chiral core model and the dissymmetric field effect. The former is proposed to be responsible for the chirality origin of the as-prepared chiral gold nanoclusters (AuNCs), and both of them are acting concurrently for the chiroptical response observed in the ligand exchange reactions, which are performed on the His enantiomer-based clusters with enantiopure thiol Pen and Cys ligands, respectively. In addition, the clusters display potential toward biological labelling due to the high photoluminescence (PL) quantum yield and remarkable cellular uptake, in spite that no chirality-dependent effects in autophagy and subcellular localization are observed in the following fluorescence imaging.

Introduction

Chirality, describing an object which is non-superimposable with its mirror image, has been extensively studied since the first reported observation of optical activity in quartz by F. J. D. Arago in 1811[1]. Along these two centuries, however, most of the investigated chiral materials correspond to organic compounds, inorganic salts and biological molecules, and although chirality at molecular level is exclusively understood, the investigation of nanoscale chirality is scarce[2, 3]. In 2000, Schaaff and Whetten did the first observation of the intense optical activity in giant gold-glutathione nanocluster compounds[4], which indicated that chiral effects are present in matter at the nanoscale. Subsequently, several endeavors have been directed toward the investigation of chiral nanostructures. More recently, there have been many reports confirming the observation of optically active nanostructures using distinct chiral molecules as protecting ligands of nanoparticles[2, 5-8].

However, so far most of the experiments[9, 10] and the theoretical work[11-13] concentrated on various types of small thiolated chiral molecules capping gold clusters due to fairly strong metal-ligand bonds, and milestones were the successful determination of a series of crystal structures[6, 14] including $Au_{102}(SR)_{44}$, $Au_{25}(SR)_{18}$, $Au_{38}(SR)_{24}$, $Au_{36}(SR)_{24}$, and $Au_{28}(SR)_{20}$. The formulated suggestions for the elusive mechanism leading to the chiroptical response of the metal core states can be divided into three major categories[2, 15]: (i) the intrinsically chiral metallic core; (ii) the dissymmetric field model; and (iii) the chiral footprint model. Although these three models have been partially supported by individual experimental results, a comprehensive understanding of the chiral origin of metal clusters is still highly desirable[16-18]. Thus, pursuing special exceptions to the gold-thiol work, such as the weakly bound phosphine-capped chiral gold clusters[19, 20] and the chiral silver clusters capped by the thiol[21, 22] or DNA molecules[23, 24], remains a worthwhile yet challenging undertaking for a deeper insight into the origin of nanoscale chirality.

In this contribution, inspired by the knowledge that the synthesis of nanoparticles involved in chiral molecules easily induces unique electronic and chiroptical response of metal nanostructures [5, 25], we present an ultra-facile one-step approach to synthesize water-soluble, monodisperse, and bluish green-emitting chiral gold nanoclusters (AuNCs), in which the enantiomers of histidine (His) serving as both a reducing agent and a protecting ligand as shown in Scheme 1. Compared to the previously-developed strategies, this synthesis method has the following advantages. First, the reaction is very rapid and mild, exempted from heating, pressuring, and special media. Second, it is a green synthesis strategy, where only two reactants of $HAuCl_4$ and the enantiomers of His are involved without extra catalysts or templates. Third, also most importantly, differing from the gold-thiol work, the His enantiomer mediated

synthesis of chiral AuNCs provide a good perspective to the understanding of the origin of nanoscale chirality. The second line of our research related to the ligand exchange toward elucidating the origin of chirality revealed the intrinsic chirality nature of these clusters, and to the best of our knowledge although the intrinsic chirality of chiral thiolate-protected gold clusters such as $Au_{102}(SR)_{44}$, $Au_{38}(SR)_{24}$, and $Au_{28}(SR)_{20}$ has been reported[6, 26-28], it is the first time that the intrinsic chirality of AuNCs protected by nitrogen-contained ligands was proposed, which has given rise to the assumption that this system could play a pivotal role in the design and application of cluster-based chiral materials.

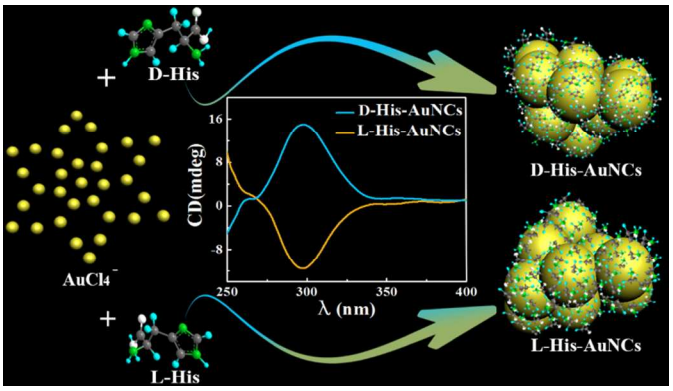

Scheme 1 Schematics of the formation of chiral AuNCs with $HAuCl_4$ and the enantiomers of histidine.

Experimental

Materials

Chemicals and solvents were reagent grade and commercially available. Chloroauric acid tetrahydrate ($HAuCl_4 \cdot 4H_2O$) was purchased from Sinopharm Chemical Reagent Co., Ltd (Shanghai, China) and dissolved in water for further use. The racemic (Rac), D- and L- enantiomeric forms of histidine (His) were all purchased from Aladdin Chemistry Co., Ltd. The D-, L-Penicillamine (Pen) and D-, L-Cysteine (Cys) were supplied from Sigma-Aldrich (Shanghai). Mili-Q purified water (18.2 MΩ cm) was used throughout the experiments. All the chemicals were used without further purification.

Apparatus

Fluorescence spectra were measured with an F-2500 fluorescence spectrophotometer (Hitachi, Tokyo, Japan)，while the UV-vis absorption spectra were recorded with a UV-3600 spectrophotometer (Hitachi, Tokyo, Japan). A Jasco J-810 circular dichroism (CD) spectroscopy (Tokyo, Japan) was used to measure the ellipticity of the clusters. The fluorescence lifetimes were recorded with a FL-TCSPC fluorescence spectrophotometer (Horiba Jobin-Yvon Inc, France). XPS measurements were performed on an electron spectrometer (VG ESCALAB MARK II) and the X-rays were from the Mg Ka line at 1253.6 eV. Photoelectrons were collected in the constant analyzer energy mode and the scan step for the whole spectrum and the Au (4f) region was 0.5 and 0.2 eV, respectively. Transmission electron microscopy (TEM) images were taken with a transmission electron microscope (JEM-1200EX). Fluorescence imaging was carried out with a DSU live-cell confocal microscope (Olympus, Japan) system with laser excitations of CY3, GFP457 and DAPI.

Synthesis of the chiral AuNCs

The optically active AuNCs were synthesized in an ultra-facile one-step blending manner. In a typical procedure, an aqueous solution of $HAuCl_4$ (1 ml, 10mM) was blended with an aqueous solution of racemic (Rac), D- and L- enantiomeric forms of His (3 ml, 0.15 M), respectively, and the mixture was kept in a glass vial at room temperature. The color of the solution turned pale yellow immediately, indicating the formation of desired AuNCs, and the mixture was incubated for 2 h for further characterization.

Ligand exchange and cellular imaging

For ligand exchange reactions, the as-prepared aqueous clusters were treated with a molar excess of enantiopure Pen or Cys, respectively (Pen : His = 4:1; Cys : His = 4:1), and the mixture was stirred at room temperature for two hour. Then the solution was dialyzed using a 1000 Da MWCO dialysis bag in double distilled water for 12 h to remove unbound thiol Pen or Cys ligands. The final solution was stored at 4 ^{0}C in refrigerator when not use. The Hep-2 cells in RPMI 1640 supplemented with 2% fetal bovine serum were added to imaging dishes (1 ml per well). Then cells were cultured for 24 h at 37 ^{0}C in a humidified 5% CO_2 atmosphere. After that, the culture medium was replaced with 1 ml RPMI 1640 containing 0.1 mg ml $^{-1}$ different kinds of cluster enantiomers and incubated at the incubator for 12h. Then the cells was washed with PBS buffer for 3 times and fixed with 4% paraformaldehyde for 30min. Finally, the bioimaging photographs were captured with a DSU live-cell confocal microscope (Olympus, Japan) system at laser excitations of DAPI (360-370 nm).

Results and discussion

Typically, blending of $HAuCl_4$ and enantiomeric forms of the His at room temperature for 2 h, respectively, results in the pale yellow solution (the inset 1 in Fig. 1a). Unlike larger nanoparticles, as shown in Fig. 1a, the clusters do not exhibit a localized surface plasmon resonance and instead, the featured absorption rises sharply below 320 nm with the maximum wavelength at 260 nm and a band edge of 460 nm, which are also different from the absorption peaks of the His and $HAuCl_4$ at 206 nm and 302 nm, respectively. The photoluminescence (PL) spectra of the clusters show an emission maximum at 498 nm when excited at 386 nm and fluorescence quantum yield is estimated as 8.96% using quinine sulfate as the reference. In line with the spectroscopic results, the strong bluish green fluorescence under 365 nm UV light irradiation can be directly

observed (the inset 2 in Fig. 1a). Meaningfully, the ellipticity of the clusters was obtained by CD spectroscopy, showing that the chirality of the His ligands is transferred to the metal core. As shown in Fig. 1b, CD spectra of the L-His-AuNCs and the D-His-AuNCs show distinct mirror images with peaks at about 298 nm, which differ from the CD scans of free L-His and D-His with a mirror image at near 214 nm (the inset picture of Fig. 1b), while the AuNCs prepared with the Rac-His produce no CD signal. Furthermore, the formed L-His-AuNCs show a negative CD signal that is opposite to the positive CD of pure L-His, and similar phenomena also occur to the D-His-AuNCs and pure D-His. Hence, we conclude that the structures of His enantiomer-based nanoclusters are stereochemically controlled and have well-defined stereostructures as common chiral molecules do. The fluorescence lifetime of L-His-AuNCs and D-His-AuNCs are 2.69 and 2.79 ns (Fig. 1c), respectively, which is in good agreement with that of gold clusters[29, 30]. Fig. 1d shows a typical transmission electron microscopy (TEM) image of the as-prepared L-His-AuNCs sample. The clusters are well dispersed and have a very narrow size distribution with an average diameter of 2.32 nm. Similar TEM images can also be obtained for the D-His-AuNCs and Rac-His-AuNCs samples. These results show direct evidence for nanocluster formation.

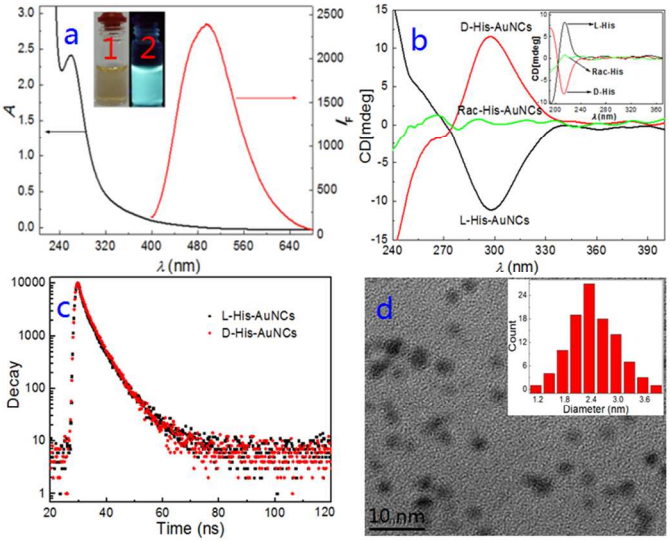

Figure 1 Characterization of the AuNCs. (a) The absorption and the fluorescence spectra of the L-His-AuNCs. The inset displays the photographs of the L-His-AuNCs solution under daylight (1) and 365 nm UV light (2); (b) CD spectra of the D-, L-, and Rac-His-AuNCs. The inset displays the CD spectra of pure D-, L-, and Rac-His; (c) The fluorescence decay of the L- and D-His-AuNCs; (d) TEM images of the L-His-AuNCs.

To maximize the chiroptic response, we optimize the synthesis of AuNCs by changing the mole ratio of His enantiomers and $HAuCl_4$. As shown in Fig. 2, with the increasing mole ratio of His enantiomers and $HAuCl_4$, the ellipticities of the AuNCs at 298 nm get increased. When the mole ratio of them is 45, it has been found that the ellipticities of L-His-AuNCs (Fig. 2a) and D-His-AuNCs (Fig. 2b) reach the maximum and do not change any more. It can be explained that when the amount of His is low, the reducing ability is not strong enough to reduce all Au^{3+},

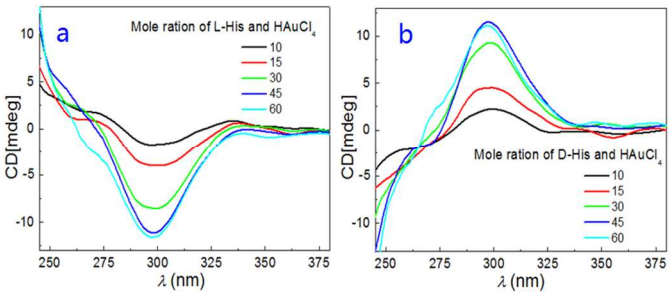

Figure 2 The dependence of the ellipticity of L-His-AuNCs (a) and D-His-AuNCs (b) on the mole ratio of His enantiomers and $HAuCl_4$, respectively.

also fail to protect the formed clusters as ligands[31]. Meaningfully, once the chiroptic cluster enantiomers such as L-His-AuNCs form, however, the negative CD signal of them remains unchanged even if the excess pure D-His are introduced and allowed to stand overnight. Also, the same behaviour occurs to the D-His-AuNCs. Generally, the dissymmetric field model assumes an achiral core either with chirality induced by chiral adsorption patterns or with chiral ligands in achiral adsorption patterns (vicinal effect), and the chiral footprint model proposes a local deformation due to the ligand-cluster interaction[2]. Thus, the plausible explanation for the unreversed CD signals of the formed cluster enantiomers is that the gold atoms, which reduced by the imidazole group in the His[31], take on the twisting atom-packing disordered structure or the chiral arrangement. That is, an inherent chiral cluster cores are proposed to be responsible for the origin of nanoscale chirality, considering that the chiral configurations were generally obtained as the lowest-energy isomers including bare, unprotected AuNCs such as Au_{28}, Au_{55} and methythiol-protected ones such as $Au_{28}(SCH_3)_{16}$, $Au_{38}(SCH_3)_{24}$[2].

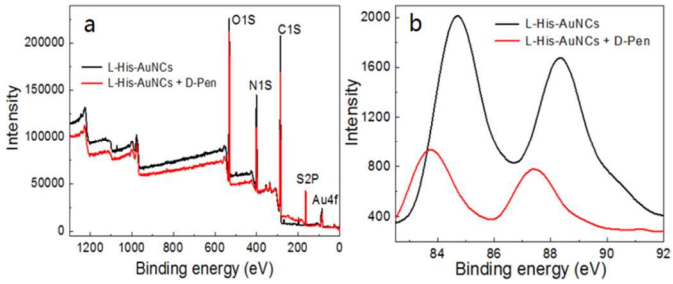

Figure 3 (a) XPS wide-scan survey of the fresh obtained L-His-AuNCs and the corresponding ligand exchange product with D-Pen, respectively; (b) the detailed XPS survey of the Au 4f region.

To confirm our claims, the ligand exchange reactions on the as-prepared chiral AuNCs were performed with enantiopure Pen and Cys, respectively. The intuitive evidences on the covering of the Pen enantiomer are provided by the XPS analysis. As shown in Fig. 3a, compared with that of alone L-His-AuNCs, the XPS wide-scan of the ligand exchange product of it with the D-Pen reveal an obvious photoelectron peak at ~164.08 eV corresponded to the binding energy of S2p[32]. More detailed XPS survey for Au 4f are displayed in Figure 3b, and the Au (4f) peak position of L-His-AuNCs is located at 84.7 eV, which

is between those of the Au (I) thiolate complex (86 eV) and Au (0) film (84 eV), similar to other literature sources[33]. The result also indicates that the products are exclusively gold nanoclusters consisting of Au^0 atoms rather than bulk gold or Au (I)-His complex. Additionally, the Au($4f_{7/2}$) peak positions for the inner Au are generally found to be monotonically shifted to lower in energy with the enhance of the core size. In contrast, the Au 4f peak positions of the ligand exchange product have been located lower in energy than that of the alone L-His-AuNCs. Similar results are also observed between the L-His-AuNCs and the corresponding ligand exchange product with the D-Cys (Figure S1). Thus the observation is clear indication for the covering of the thiol Pen and Cys ligands on the surface of the AuNCs through strong metal-thiol bonds. Further, the chiral thiol ligands bound to the surface of the Au core through strong metal-thiol bonds were confirmed by the absence of the absorption band at ν(S-H) = 2526 cm^{-1} in the FTIR spectra of the as-prepared cluster sample (Figure S2).

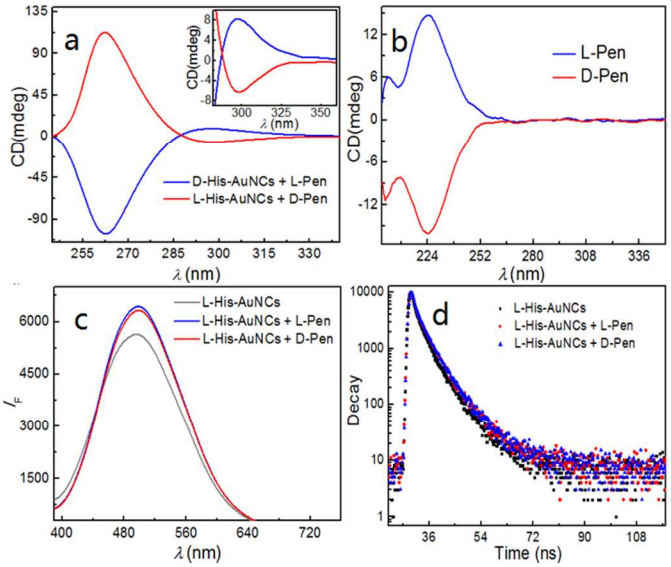

Figure 4 (a) CD spectra of the D- and L-His-AuNCs after surface passivation with the enantiomers of Pen. Inset is the magnified spectra in the wavelength region of 280-360 nm. (b) CD spectra of pure D-Pen and L-Pen. (c) The emission spectra of L-His-AuNCs and the ligand exchange products with the D/L-Pen. (d) Time-resolved fluorescence decays of L-His-AuNCs and the ligand exchange products with the D/L-Pen.

Upon exchange with Pen, intense CD signals located at 262 nm can be observed with opposite sign for clusters covered by the enantiomers of Pen as shown in Fig. 4a. These CD spectra are considerably different from the one of free Pen, which shows CD signals at 225 nm (Fig. 4b). The appearance of intense CD signals is a clear indication of the novel optical activity due to the surface passivation of the enantiomers of Pen. It is also evidenced by the fact that the steady-state fluorescence intensities enhance and the fluorescence lifetimes prolong (from 2.69 to 2.92 ns) as shown in Fig. 4c and 4d, respectively. Additionally, a further observation is that the CD signals at 298 nm nearly remain unchanged after exchange with the D/L-Pen as shown in the inset picture of Fig. 4a, which is completely different from the observation that the optical activity of gold clusters is reversed when the thiolate-for-thiolate ligand exchange was performed[10]. It is confirmed that the intrinsically chiral metallic core is responsible for the chirality of His enantiomer-based clusters, showing that the chiral arrangement of gold atoms in the cluster core could withstand the driving force and the lattice geometries of these cores would not be geometrically distorted by the covering of the Pen enantiomers. Generally, for the chiral footprint model, the adsorption of chiral molecules tends to a preferential crystal facet and results in the chiral stress of local surface metal atoms[10], and according to the observation described above, it seems unlikely and would not fit to account for the CD response observed in our case. Therefore, the new appeared CD band should be ascribed to the chiral perturbation of the cluster core using the dissymmetrical field model.

To further demonstrate this point, another chiral ligand Cys is used under identical reaction conditions. The CD spectra show the development of optical activity with a mirror image relationship for the two enantiomers with bands at 259 nm and 298 nm (Figure S3a). Again these CD spectra are different from the ones of neat Cys (Figure S3b). In spite of bearing some similarity, also they are different from the CD spectra obtained by the exchange with D/L-Pen, which shows that the optical activity induced by the ligand exchange reaction is ligand dependent. Similarly, the enhancement of the steady-state fluorescence intensity and the prolonging of the fluorescence lifetime (from 2.69 to 2.93 ns) also occur (Figure S3c and 3d). Interestingly, the CD signals at 298 nm nearly remain unchanged after exchange with the D/L-Cys (the inset of Figure S2a), supporting the contention that the intrinsically chiral core is responsible for the chirality of His enantiomer-based clusters.

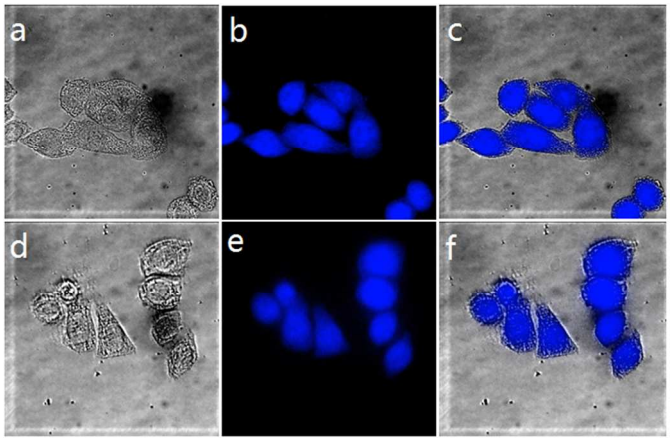

Figure 5 Confocal microscopy images of Hep2 cells treated with L-His-AuNCs (a-c) and D-His-AuNCs (d-f), respectively. Left, Differential interference contrast (DIC) images (a, d); middle, PL images (b, e); right, merged images (c, f). Scale bars: 20 μm.

Although it is well-known that chirality is paramount in both structures and functions of bio-organisms and surface modification of nanoparticles endows them with unique

biological functionalities, the impact of the chirality at the nanoscale on living organisms has been largely neglected. Recently, a meaningful work is that the effects of quantum dots (QDs) capped with different chiral forms of the tripeptide glutathione (GSH) on cytotoxicity and induction of autophagy were examined, in which the activation of autophagy was chirality-dependent, with L-GSH-QDs being more effective than D-GSH-QDs[34]. Therefore, in order to know whether the differences in autophagy and/or subcellular localization exist between the L-His-AuNCs and the D-His-AuNCs, the Hep-2 cells are exposed to the same concentrations of the L-His-AuNCs and D-His-AuNCs and the cell imaging is followed. Thanks to the high PL quantum yield and remarkable cellular uptake, as shown in Fig. 5, nanoclusers can be clearly seen in the cytoplasm of cells by means of confocal microscope, indicating that they can be used as the fluorescence dye to stain cells and display the potential in biological labelling. But, no differences in autophagy and subcellular localization are observed between the L-His-AuNCs and the D-His-AuNCs, which may also be viewed as the indirect evidence that the chirality originate from the cluster core rather than the particle surface. Subsequently, the Hep-2 cells are treated with the ligand exchange products of D/L-His-AuNCs with D/L-Pen and D/L-Cys, respectively, and contrary to our expectation, still no differences in autophagy or subcellular localization for the ligand-exchanged cluster enantiomers are observed (Figure S4 and Figure S5). Although the results do not demonstrate differential effects associated with the chirality, we are not discouraged to explore the chirality transfer from molecular scale to nanometer scale and further extend the chirality-dependent applications.

Conclusions

In summary, the strongly emitting chiral AuNCs are prepared using an ultra-facile one-step approach, in which enantiomers of His serve as both a reducing agent and a stabilizing ligand. No CD spectra can be induced in an optically inactive racemic mixture of chiral clusters or even reversed when the chiroptic clusters covered by one enantiomer are exposed to the opposite one. Hence, an intrinsically chiral metal core model is proposed to elucidate the origin of the optical activity. The contention is further supported by performing the ligand exchange reactions on the as-prepared chiral AuNCs with enantiopure thiol Pen and Cys ligands, respectively, and at this time, both intrinsically chiral metal core and dissymmetrical field model are acting concurrently for the CD response observed in the ligand exchange products. In addition, the clusters display potential toward biological labelling due to the high PL quantum yield and remarkable cellular uptake, in spite that no chirality-dependent effects in autophagy and subcellular localization are observed in the application of chiral cluster enantiomer-based cell imaging.

Acknowledgements

All authors herein greatly appreciate the financial support from the National Natural Science Foundation of China (NSFC, 21205096), the Fundamental Research for the Central Universities (XDJK2014B023), and the Program for Innovative Research Team in University of Chongqing (2013).

Notes and references

[a]*Key Laboratory of Luminescent and Real-Time Analytical Chemistry, Ministry of Education, College of Pharmaceutical Sciences, Southwest University, Chongqing 400715*

[b]*College of Horticulture and Landscape Architecture, Southwest University, Chongqing 400715*

†To whom all correspondence should be addressed. Tel: 86-23-68251225; E-mail: lzdzhy@swu.edu.cn.

Electronic Supplementary Information (ESI) available: [details of any supplementary information available should be included here]. See DOI: 10.1039/b000000x/

1. L. D. Barron, Molecular Light Scattering and Optical Activity, Cambridge University Press, Cambridge, 2004.
2. C. Noguez, I. L. Garzon, *Chem. Soc. Rev.*, **2009**, *38*, 757.
3. Y. S. Xia, Y. L. Zhou, Z. Y. Tang, *Nanoscale*, **2011**, *3*, 1374.
4. T. G. Schaaff and R. L. Whetten, *J. Phys. Chem. B*, **2000**, *104*, 2630.
5. M. Farrag, M. Tschurl, U. Heiz, *Chem. Mater.*, **2013**, *25*, 862.
6. S. Knoppe, T. Burgi, *Acc. Chem. Res.*, **2014**, *47*, 1318.
7. M. P. Moloney, Y. K. Gunko, J. M. Kelly, *Chem. Commun.*, **2007**, *38*, 3900.
8. T. Nakashima, Y. Kobayashi, T. Kawai, *J. Am. Chem. Soc.*, **2009**, *131*, 10342.
9. H. Yao, T. Fukui, K. Kimura, *J. Phys. Chem. C* **2007**, *111*, 14968.
10. C. Gautier, T. Brugi, *J. Am. Chem. Soc.* **2008**, *130*, 7077.
11. L. Garzon, J. A. Reyes-Nava, J. I. Rodryguez-Hernandez, I. Sigal, M. R. Beltran, K. Michaelian, *Phys. Rev. B* **2002**, *66*, 073403.
12. Lopez-Acevedo, J. Akola, R. L. Whetten, H. Gronbeck, H. Hakkinen, *J. Phys. Chem. C*, **2009**, *113*, 5035.
13. C. M. Aikens, *J. Phys. Chem. A*, **2009**, *113*, 10811.
14. P. D. Jadzinsky, G. Calero, C. J. Ackerson, D. A. Bushnell, R. D. Kornberg, *Science*, **2007**, *318*, 430.
15. T. Molotsky, T. Tamarin, A. B. Moshe, G. Markovich, A. B. Kotlyar, *J. Phys. Chem. C*, **2010**, *114*, 15951.
16. U. Tohgha, K. K. Deol, A. G. Porter, S. G. Bartko, J. K. Choi, B. M. Leonard, K. Varga, J. Kubelka, G. Muller and M. Balaz, *ACS Nano*, **2013**, *7*, 11094.
17. V. Humblot, S. Haq, C. Muryn, W. A. Hofer and R. Raval, *J. Am. Chem. Soc.* **2001**, *124*, 503.
18. M.-R. Goldsmith, C. B. George, G. Zuber, R. Naaman, D. H. Waldeck, P. Wipf and D. N. Beratan, *Phys. Chem. Chem. Phys.* **2006**, *8*, 63.
19. X. K. Wan, S. F. Yuan, Z. W. Lin, Q. M. Wang, *Angew. Chem.* **2014**, *126*, 1967.
20. Y. Yanagimoto, Y. Negishi, H. Fujihara, T. Tsukuda, *J. Phys. Chem. B* **2006**, *110*, 11611.
21. N. Nishida, H. Yao, K. Kimura, *Langmuir*, **2008**, *24*, 2759.
22. N. Cathcart, P. Mistry, C. Makra, B. Pietrobon, N. Coombs, M. Jelokhani-Niaraki, V. Kitaev, *Langmuir*, **2009**, *25*, 5840.
23. G. Shemer, O. Lomanets, G. Markovich, T. Molotsky, I. Lubitz, A. B. Kotlyar, *J. Am. Chem. Soc.* **2006**, *128*, 11006.
24. T. Molotsky, T. Tamarin, A. B. Moshe, G. Markovich, A. B. Kotlyar, *J. Phys. Chem. C* **2010**, *114*, 15951.
25. Z. Wu, C. Gayathri, R. R. Gil, R. Jin, *J. Am. Chem. Soc.* **2009**, *131*, 6535.
26. P. D. Jadzinsky, G. Calero, C. J. Ackerson, D. A. Bushnell, R. D. Kornberg, *Science*, **2007**, *318*, 430.
27. Lopez-Acevedo, H. Tsunoyama, T. Tsukuda, H. Hakkinen, C. M. Aikens, *J. Am. Chem. Soc.* **2010**, *132*, 8210.
28. C. Zeng, T. Li, A. Das, N. L. Rosi, R. Jin, *J. Am. Chem. Soc.* **2013**, *135*, 10011.

29. R. C. Price, and R. L. Whetten, *J. Am. Chem. Soc.* **2005**, *127*, 13750.
30. H. W. Duan, and S. M. Nie, *J. Am. Chem. Soc.* **2007**, *129*, 2412.
31. X. Yang, M. M. Shi, R. J. Zhou, X. Q. Chen, H. Z. Chen, *Nanoscale*, **2011**, *3*, 2596.
32. M. Thompson, J. Whelan, D. J. Zemon, B. Bosnich, E. I. Solomon, H. B. Gray, *J. Am. Chem. Soc.* **1979**, *101*, 2482.
33. Y. Negishi, K. Nobusada, and T Tsukuda, *J. Am. Chem. Soc.* **2005**, *127*, 5261.
34. Y. Y. Li, Y. L. Zhou, H. Y. Wang, S. Perrett, Y. L. Zhao, Z. Y. Tang, G. J. Nie, *Angew. Chem. Int. Ed.*, **2011**, *50*, 5860.

